CSCanada
Advances in Petroleum Exploration and Development
Vol. 3, No. 1, 2012, pp. 33-37
DOI:10.3968/j.aped.1925543820120301.155

ISSN 1925-542X [Print]
ISSN 1925-5438 [Online]
www.cscanada.net
www.cscanada.org

Numerical Simulation of Fracture Width Influencing Law on Reservoir Permeability after Fracturing

YANG Ningning[1,*]

[1] Institute of Drilling Technology, Shengli Petroleum Administration Bureau, Dongying 257017, China.
[*]Corresponding author.

Received 9 January 2012; accepted 10 February 2012

Abstract
Based on the fluid-solid coupling theory in porous media, a finite element simulation model for dynamic fracture creation is established and the finite element simulation program is developed, and then relevant finite element simulation is conducted on the permeability distribution under the simultaneous influence of fracture creation and pressure-released production. Research results demonstrate that the permeability distribution law after fracturing is similar for fractures with different widths, and the permeability distribution shapes in ellipse. When the maximal fracture width is greater than or equal to 6mm, the influence region on the permeability increases apparently with the increment of fracture width, so does the influence in the vicinity of the wellbore. The fracture creation and pressure-released production alternately dominates the alteration of permeability in different regions. Dynamic fracture creation plays a more important role in permeability alteration within the region less than 5m away from the wellbore axis. The larger for the fracture width, the more sensitive for the permeability alteration gradient is observed in the region in the vicinity of the wellbore. In the region 20m away from the wellbore axis, the pressure-released production affect more apparently since dynamic fracture creation has a negligible effect in the region.

Key words: Fluid-solid coupling; Permeability; Fracture; Wellbore; Simulation

YANG, N. N. (2012). Numerical Simulation of Fracture Width Influencing Law on Reservoir Permeability after Fracturing. *Advances in Petroleum Exploration and Development*, *3*(1), 33-37. Available from: URL: http://www.cscanada.net/index.php/aped/article/view/j.aped.1925543820120301.155
DOI: http://dx.doi.org/10.3968/j.aped.1925543820120301.155

Nomenclature
κ = the reservoir permeability
μ= the oil phase viscosity
C_t = the total compressibility
ε_v= the volumetric strain
σ_{ij}= the effective stress component
f_i = the volumic force
α= the Biot's poroelastic constant
a = the fitting coefficient of experiment
b = the fitting coefficient of experiment
σ = the effective stress

INTRODUCTION
The low permeability reservoir commonly shows relatively stronger stress sensitivity, and the petrophysical parameters will change with the suffered effective stress for reservoir rock frame[1-5].The artificial fracture creation in hydraulic fracturing and the pressure-released production will impose specified additional stress on the reservoir rock, which result in the change of formation pore configuration and reservoir permeability. Based on the fluid-solid coupling theory in porous media, a finite element simulation on dynamic fracture creation and pressure-released production is conducted, and the distribution law of permeability is quantitatively studied under the influence of both fracture creation and pressure-released production, and the effect of the dynamic creation of fracture with different widths is analyzed.

1. BASIC EQUATIONS OF FLUID-SOLID COUPLING THEORY IN POROUS MEDIA
The fluid-solid coupling mathematical model basically

consists of three parts, including the fluid-flow equation, stress-deformation equation and auxiliary equation [6-10]. The single phase flow equation is adopted in the seeping field, and a linear elastic constitutive equation is introduced in the stress field.

The fluid-flow equation is:

$$\frac{K}{\mu C_t}\nabla^2 p - \frac{1}{C_t}\frac{\partial \varepsilon_v}{\partial t} = \frac{\partial P}{\partial t} \quad (1)$$

The balance equation of stress-deformation can be expressed as:

$$\frac{\partial \sigma_{ij}}{\partial x_j} + \alpha\frac{\partial P}{\partial x_i} + f_i = 0 \quad (2)$$

Liu Jianjun[5] have experimentally concluded that the permeability of low permeable reservoir is a function of effective stress (σ).

$$K = a \cdot e^{-bs} \quad (3)$$

In addition to the above-mentioned basic equations, the boundary condition and initial condition of the seeping field and stress field are also required for the solution of the fluid-solid coupling model. With respect to the seeping field, the commonly used boundary condition is either the constant pressure or the constant flow rate. With respect to the stress field, the commonly used boundary condition is either the stress or the displace [9-10].

Based on the fluid-solid coupling theory, the relevant finite element program is developed with the software of FEPG (Finite Element Program Generator), and the finite element model of dynamic fracture creation is analyzed.

2. ESTABLISHMENT OF DYNAMIC FRACTURE CREATION MODEL

Two basic assumptions adopted in the model are as follows: (1) the assumption of plain strain is introduced, and (2) the double wing of the hydraulic vertical fracture is symmetrical. A quarter of the model is simulated and analyzed because of the structural symmetry of the model. The size of the model is 300m×300m, the basic parameters of finite element simulation are presented in Table 1.

Table 1
Basic Parameters of Finite Element Simulation

Radius of bore hole /m	Maximum horizontal in-situ stress /MPa	Minimal horizontal in-situ stress /MPa	Pore pressure /MPa	Young's modulus / MPa	Poisson ratio
0.15	45	32	20	2.5×10^4	0.25
Biot's poroelastic constant	Reservoir permeability /m^2	Oil phase viscosity /Pa • s	Total compressibility /Pa^{-1}	Coefficient of sensitivity(a) /mD	Coefficient of sensitivity(b)
0.8	20×10^{-15}	3×10^{-3}	3.0×10^{-10}	97.7	0.0675

The finite element model of dynamic fracture creation is shown in Fig.1, and the geometry of hydraulic fracture is wedge. The fracture length is 120m, and the fracture width at the fracture tip is 0mm.The dynamic creation of fractures with width of 3mm, 4mm, 6mm, 8mm and 10mm are simulated.

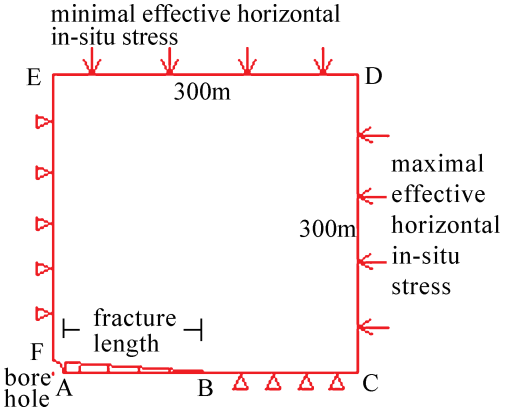

Figure 1
Schematic Diagram of the Dynamic Fracture Creation Model

The radius of borehole is very little compared with the size of the model, so the borehole can be simplified into a point in the simulation. And then the boundary condition and the initial condition are applied to the seeping field and the stress field.

The simulation without the dynamic fracture creation is also conducted. The edges of AB and BC are under the same boundary condition of displace constraint, the maximal effective horizontal stress is imposed on the edge of CD, and the minimal effective horizontal stress is imposed on the edge of DE. The flow conductivity of hydraulic fracture is assumed to be infinite, the flowing pressure of fracture surface is setup up to be 17MPa in the pressure-released production, and the initial value of pore pressure is setup to be 20MPa.

The formation time of fracture is assumed to be 30 minutes, the edge of AB is setup to be under the condition of dynamic displacement in the process of dynamic fracture creation, and the edge of AB is under the condition of displacement constraint after fracturing. With respect to the seeping field, the edge of AB is under the condition of dynamic flowing pressure. The value of

flowing pressure of the edge of AB is setup to be 23MPa during the dynamic fracture creation, and it will become into 17MPa (producing pressure) after fracturing.

The fluid-solid coupling model is solved by explicitly iterative calculation. After the calculation of the seeping field is completed, the increment of pore pressure is transferred to the stress field, the alteration of the effective stress induces change of the reservoir permeability, and then the updated permeability is used again in seeping field. Considering the simultaneous influence of fracture creation and pressure-released production, the boundary conditions of the coupling field and the dynamic parameters are regenerated at each time step.

3. DISTRIBUTION LAW OF RESERVOIR PERMEABILITY UNDER THE INFLUENCE OF FRACTURE CREATION

The simulation without the dynamic fracture creation is also conducted. Research results demonstrate that the value of permeability in the vicinity of the fracture surface declined from 20mD to 18mD, and the percent of permeability decrease is 10%. The permeability distribution under the simultaneous influence of fracture creation and pressure-released production is showed in Figs.2 through 6, and the unit of permeability is mD in this figures. The value of permeability near wellbore and fracture surface is obviously less than 18mD, and the further decrease of permeability originates from the dynamic fracture creation.

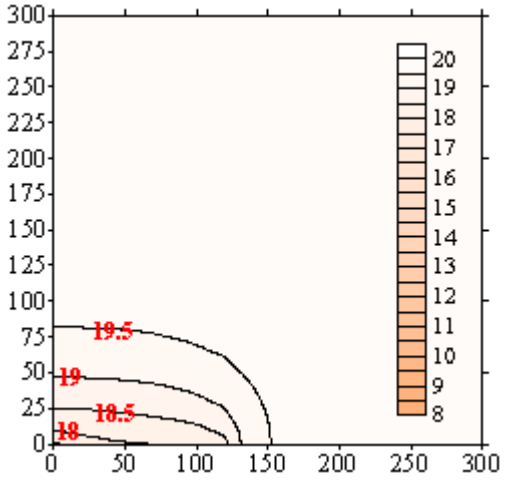

Figure 2
Permeability Distribution for Fracture with Maximal Width of 3mm

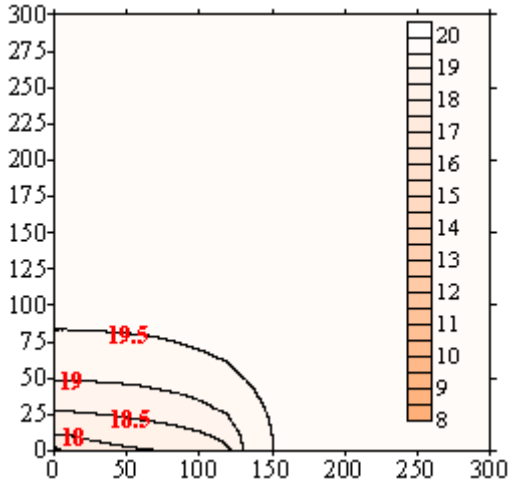

Figure 3
Permeability Distribution for Fracture with Maximal Width of 4mm

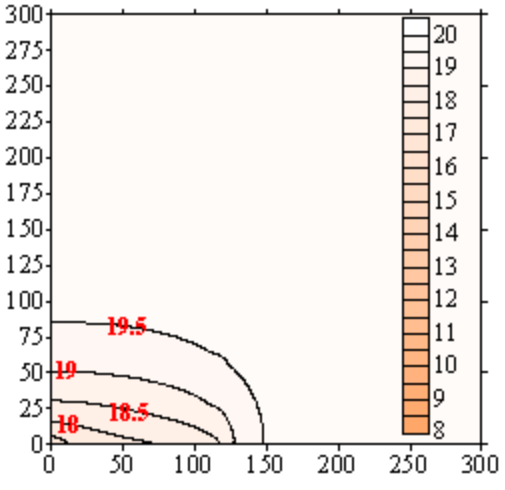

Figure 4
Permeability Distribution for Fracture with Maximal Width of 6mm

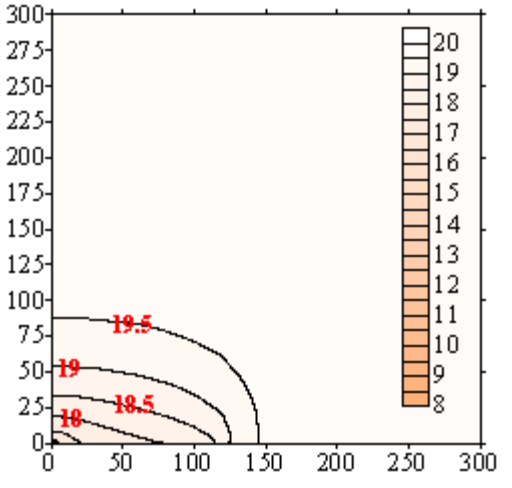

Figure 5
Permeability Distribution for Fracture with Maximal Width of 8mm

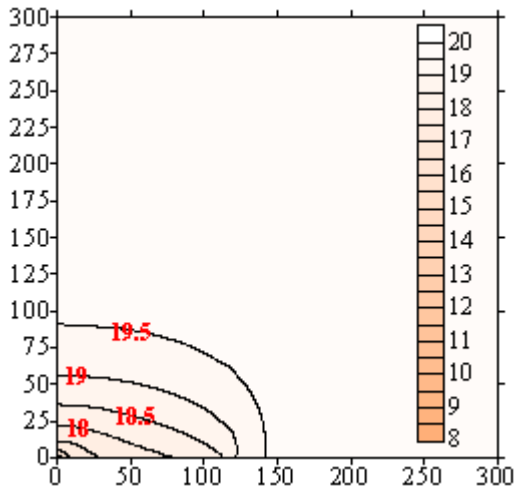

Figure 6
Permeability Distribution for Fracture

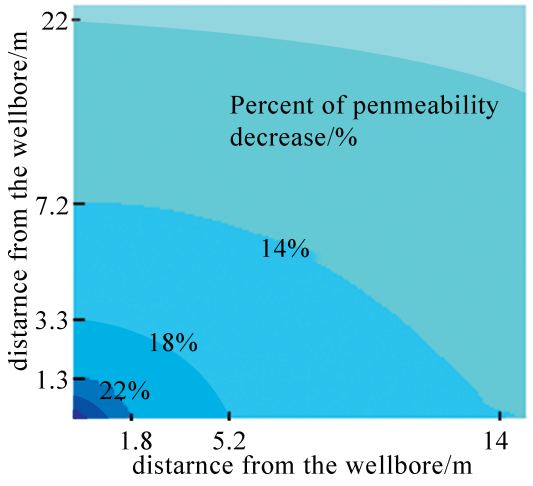

Figure 7
Effect on Permeability Around the Wellbore with Maximal Width of 10mm

Figs.2 to 6 show that the permeability distribution law is similar for wedge fractures with the same length and different widths, and the permeability distribution shapes in ellipse. The influence region along the fracture surface by fracture creation has a negligible increase with the increment of the fracture width. When the maximal fracture width is greater than or equal to 6mm, the influence region on the permeability increases apparently with the increment of fracture width, so does the influence in the vicinity of the wellbore.

When the maximal fracture width is greater than or equal to 6mm, an occurrence of the apparent influence region near wellbore is observed. An example of fracture with width of 10mm is used to demonstrate the permeability distribution near wellbore, and Fig. 7 shows the permeability distribution near wellbore. Fig. 7 shows that the permeability distribution also shapes in ellipse under the influence of dynamic fracture creation. Moreover, the more adjacent to the wellbore, the more sensitive for the permeability alteration is observed. The fracture creation has obvious influence on permeability in the region less than 4m away from the wellbore, and the percent of permeability decrease in this region is even about 50%.

Fig.8 shows the percent of permeability decrease along the boundary of fracture (the edge of AB in Fig.1), and Fig.9 shows the percent of permeability decrease along the vertical boundary of fracture model (the edge of EF in Fig.1).

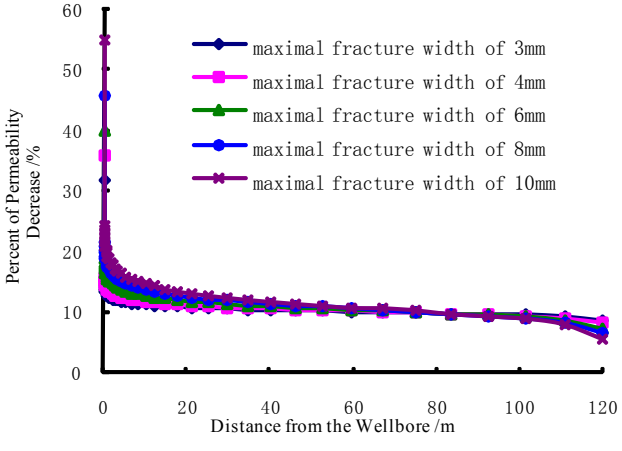

Figure 8
Effect on Permeability Along the Boundary of Fracture

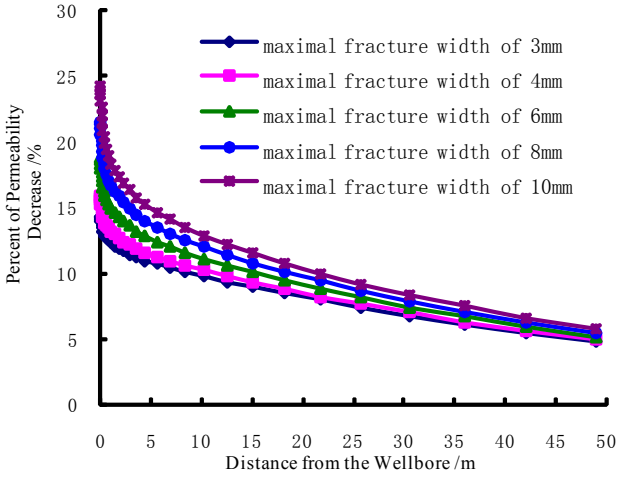

Figure 9
Effect on Permeability Along the Vertical Boundary of Fracture Model

Fig.8 and Fig.9 show the obvious decrease of reservoir permeability under the simultaneous influence of fracture creation and pressure-released production, and the fracture creation and pressure-released production alternately dominates the alteration of permeability in different regions. With respect to the fractures with different widths, the fracture creation apparently dominates the change of permeability in the region near the wellbore and the fracture surface. Moreover, the more adjacent to the wellbore, the more apparent for the effect of fracture creation is observed. Dynamic fracture creation plays a more important role in permeability alteration within the region less than 5m away from the wellbore. The larger for the fracture width, the more sensitive for the permeability alteration gradient is observed in the region near wellbore. In the region 5m away from the wellbore, the effect of fracture creation decreases sharply with the increment of the distance from the wellbore. In the region 20m away from the wellbore, the pressure-released production affect more apparently since dynamic fracture creation has a negligible effect in the region.

CONCLUSIONS

(1) Based on the fluid-solid coupling theory in porous media, a finite element simulation model for dynamic fracture creation is established, the relevant finite element program is developed with the software of FEPG.

(2) The permeability distribution after fracturing shapes in ellipse for fractures with different widths. When the maximal fracture width is greater than or equal to 6mm, the influence region on the permeability increases apparently with the increment of fracture width, so does the influence in the vicinity of the wellbore.

(3) The fracture creation and pressure-released production alternately dominates the alteration of permeability in different regions. Dynamic fracture creation plays a more important role in permeability alteration within the region less than 5m away from the wellbore. The larger for the fracture width, the more sensitive for the permeability alteration gradient is observed in the region in the vicinity of the wellbore. In the region 20m away from the wellbore axis, the pressure-released production affect more apparently since dynamic fracture creation has a negligible effect in the region.

REFERENCES

[1] Tran, D., Nghiem, L., & Buchanan, L. (2005). An Overview of Iterative Coupling Between Geomechanical Deformation and Reservoir Flow. *SPE97879*.

[2] Belhaj, H. A., Ryan, R. J., Nouri, A. M., et al (2004). A New Coupled Fluid Flow/Stress Model for Porous Media Behavior: Numerical Modeling and Experimental Investigation. *SPE90265*.

[3] Tran, D., Settari, A., & Nghiem, L. (2004). New Iterative Coupling Between a Reservoir Simulator and a Geomechanics Model. *SPE 88989*.

[4] Onaisi, A., Samier, P., & Koutsabeloulis, N., et al (2002). Management of Stress Sensitive Reservoirs Using Two Coupled Stress-Reservoir Simulation Tools: ECL2VIS and ATH2VIS. *SPE78512*.

[5] Liu, J. J., Liu X. G., & Hu, Y. R. (2002). Study of Fluid-Solid Coupling Flow in Low Permeablable Oil Reservoir. *Chinese Journal of Rock Mechanics and Engineering*, *21*(1), 88-92.

[6] Zhang, G. Q., Chen, M., & Jin, Y. (2005). Three-Dimensional Model and Procedures for Prediction of Sand Production in Gas Reservoirs. *Chinese Journal of Geotechnical Engineering*, *27*(2), 198-201.

[7] Xu, X.R., & Fan, X. P. (2002). Math Simulation on Coupled Fluid Flow and Geomechanics for Multiple Phases Reservoir. *Chinese Journal of Rock Mechanics and Engineering*, *21*(1), 93-97.

[8] Xue, S. F., Tong, X. H., & Yue, B. Q., et al (2000). Progress of Seepace-Rock Mass Coupling Theory and Its Application. *Journal of the University of Petroleum, China(Edition of Natural Science)*, *24*(2), 109-114.

[9] Liu J. J., & Feng, X. T. (2003). Advance of Studies on Thermo-Hydro-Mechanical Interaction in Oil Reservoir in China. *Rock and Soil Mechanics*, *24*(Sup), 645-650.

[10] Liang, B., Sun, K. M.,& Xue Q. (2001). The Research of Fluid-Solid Coupling in the Ground Engineering. *Journal of Liaoning Technical University (Natural Science)*, *20*(2), 129-134.

